

Genome-wide CRISPR screens identify ferroptosis as a novel therapeutic vulnerability in acute lymphoblastic leukemia

Marie-Eve Lalonde,¹ Marc Sasseville,¹ Anne-Marie Gélinas,¹ Jean-Sébastien Milanese,¹ Kathie Béland,² Simon Drouin,¹ Elie Haddad² and Richard Marcotte¹

¹Human Health Therapeutics Research Center, National Research Council Canada and ²Centre Hospitalier Universitaire Sainte-Justine, Université de Montréal, Montréal, Quebec, Canada

Correspondence: R. Marcotte
richard.marcotte@nrc-cnrc.gc.ca

Received: February 2, 2022.

Accepted: September 13, 2022.

Prepublished: September 22, 2022.

<https://doi.org/10.3324/haematol.2022.280786>

©2023 Ferrata Storti Foundation

Published under a CC-BY license 

Abstract

Acute lymphoblastic leukemia (ALL) is the most frequent cancer diagnosed in children. Despite the great progress achieved over the last 40 years, with cure rates now exceeding 85%, refractory or relapsed ALL still exhibit a dismal prognosis. This poor outcome reflects the lack of treatment options specifically targeting relapsed or refractory ALL. In order to address this gap, we performed whole-genome CRISPR/Cas drop-out screens on a panel of seven B-ALL cell lines. Our results demonstrate that while there was a significant overlap in gene essentiality between ALL cell lines and other cancer types survival of ALL cell lines was dependent on several unique metabolic pathways, including an exquisite sensitivity to GPX4 depletion and ferroptosis induction. Detailed molecular analysis of B-ALL cells suggest that they are primed to undergo ferroptosis as they exhibit high steady-state oxidative stress potential, a low buffering capacity, and a disabled GPX4-independent secondary lipid peroxidation detoxification pathway. Finally, we validated the sensitivity of B-ALL to ferroptosis induction using patient-derived B-ALL samples.

Introduction

Acute lymphoblastic leukemia (ALL) is the most prevalent cancer during childhood, representing nearly 80% of all cancer in this age group.¹ Treatment protocols have greatly improved over the last 30 years, such that the survival rate reaches >85%.² Despite this therapeutic success, the prognosis for relapsed patients remains dismal with a less than 50% 5-year survival, still making ALL the second highest cause of death by disease amongst children in Canada and in the US. In addition, up to 65-70% of pediatric ALL survivors will suffer from long-term debilitating or even life-threatening treatment related sequelae.^{3,4} Hence, novel therapeutic avenues that are both more effective at achieving long-term remission while eliciting less acute long-term toxicities than current treatment regimen are required to treat these patients.

Recent advances in the use of clustered regularly-interspaced short palindromic repeat (CRISPR)/Cas9 technology has revolutionized functional genomics and the analysis of gene function in mammalian cells with its precision, ease of use, speed, and versatility. Whole-

genome bulk pooled CRISPR screens, using multiple single-guide RNA (sgRNA) targeting each human gene in a single CRISPR library, have allowed the identification of genes implicated in processes underlying phenotypic read-outs such as proliferation and survival in hundreds of tumoral cell lines.⁵⁻⁷ These large datasets revealed panels of core essential and pan-cancer genes and unraveled key players required for cell viability/proliferation in cell lines derived from multiple histotypes. Although ALL is a common form of cancer, very few ALL cell lines have been previously screened by large dropout screen studies.⁵⁻⁷ This is likely explained by the difficulty in infecting pre-B and T lymphocytes with lentiviruses, a technical requirement for performing whole-genome CRISPR screens.

In this report, we performed whole-genome dropout CRISPR screens of seven B-ALL cell lines. These screens revealed a surprisingly large subset of essential genes unique to ALL cell survival that were not reported to be core essential genes in previous studies.⁶⁻⁸ These B-ALL-enriched genes were implicated in different cellular pathways and functions, many of which were associated directly or indirectly to ferroptosis. In recent years, this

non-apoptotic pathological cell death has gained increasing attention in cancer research, particularly for its potential tumor suppressor function that could be exploited for neoplastic disease treatment.^{9–11} By using different cellular and molecular biology approaches, we validate that B-ALL cell lines have an exquisite vulnerability to ferroptosis induction. This sensitivity is illustrated by the extreme responsiveness of cells to glutathione peroxidase 4 (GPX4) inhibition, but also to other pathways that regulate GPX4 activity. We also show that this sensitivity is rescued by exogenous expression of FSP1, a recently characterized ferroptosis inhibitor^{12,13} that we found to be poorly expressed, not only in B-ALL cells, but in leukemias in general. Finally, we demonstrate that this acute sensitivity to ferroptosis induction is also observed in a panel of B-ALL patient-derived tumor samples.

Methods

B-acute lymphoblastic leukemia cell screens

B-ALL cells were infected with Cas9-2A-blast lentivirus followed by selection with 5–15 $\mu\text{g}/\text{mL}$ blasticidin (InvivoGen, CA). Cells were tested for Cas9 activity using the reporter assay described in Tzelepis *et al.*¹⁴ Cas9-expressing B-cell stable pools were transduced at 0.3 multiplicity of infection (M.O.I) with the pLKV2 whole-genome human library (Addgene # 67989), at 300-fold representation in triplicate (~30 million cells per replicate). Twenty-four hours (h) post infection, cells were centrifuged and resuspended in fresh media + 0.5–7.5 $\mu\text{g}/\text{mL}$ puromycin (Gibco™). Forty-eight h post puromycin addition, cells were counted with Vi-Cell™ XR (Beckman Coulter, IN) and 30 million cells were pelleted per replicate for T0 time points. M.O.I. evaluation was done using CellTiter-Glo® (Promega, WI) and measured using a Synergy 2 luminometer (BioTek®). Thirty million cells per replicate were plated in culture and left for about 14 doublings with regular passage (2–4 days). After 14 doublings, 30 million cells per replicate were pelleted for the final time points (Tf).

Screen +/- ferrostatin

REH and SEM Cas9 pools were screened as described above, except that each pool was screened +/- 4 μM ferrostatin in parallel. Ferrostatin and puromycin were added 24 h post transfection. Analysis was performed using MAGeCK Maximum Likelihood Estimation (MLE) algorithm with combined data from two cell lines and the MAGeCK-Flute R package (version 1.4.3).⁵⁸

Ethic committee approval

All experiments performed with patient-derived xenografts (PDX) were approved by Ste-Justine Hospital Ethic Committee, under approbation #F9-25754.

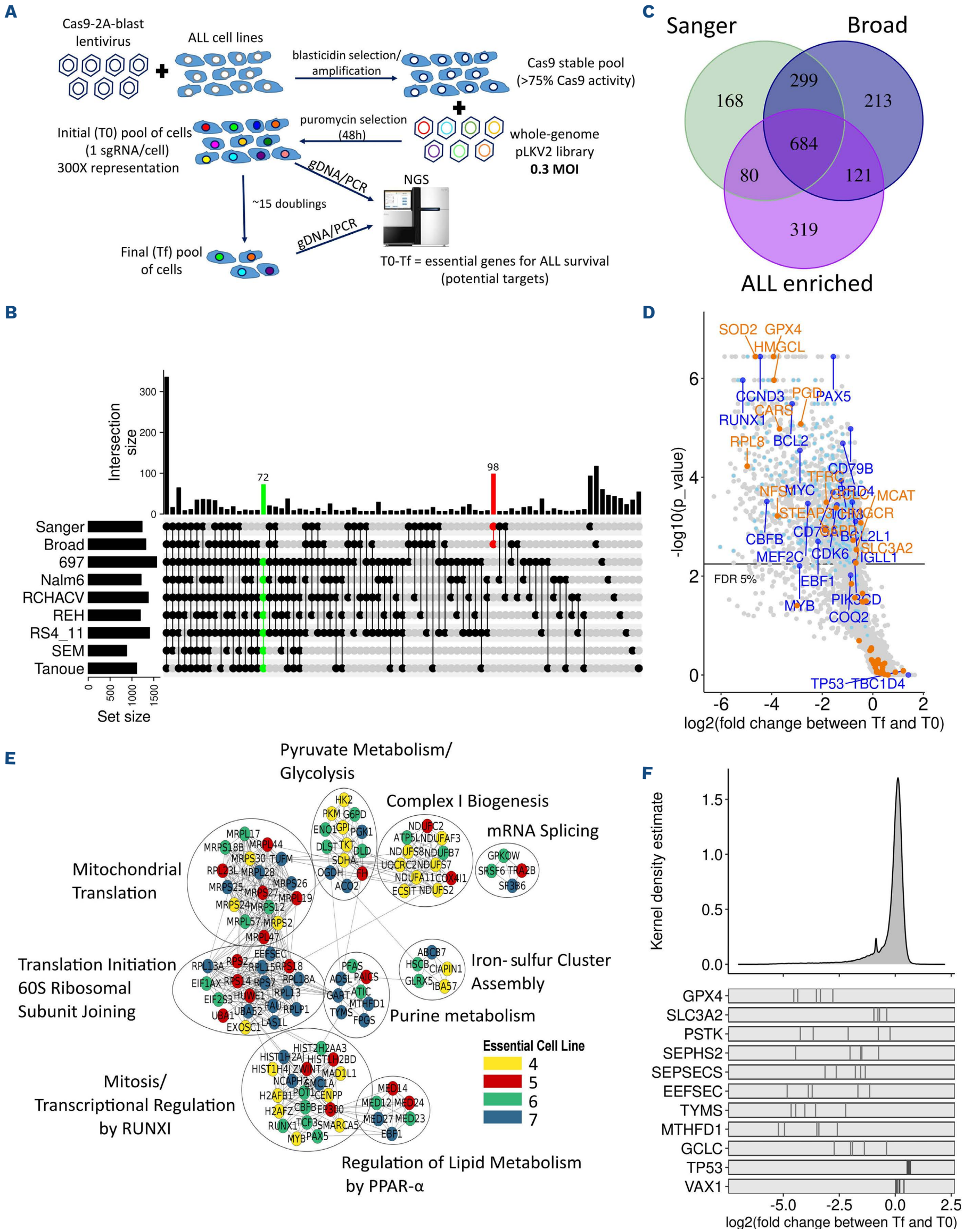
Results

Whole-genome CRISPR screens of B-acute lymphoblastic leukemia cell lines

In order to identify genes that are essential for B-ALL cells, we performed whole-genome pooled dropout CRISPR screens using a two-vector system (Figure 1A).¹⁴ First, a stable pool of Cas9-expressing cells was established for each cell line. This preliminary step was limiting for many ALL cell lines, since several pools did not reach the 75% Cas9 activity threshold required for further screening (*Online Supplementary Table S2*). For some of these cell lines, Cas9 activity decreased rapidly after blasticidin selection, particularly in T-ALL cell lines (*data not shown*), suggesting that constitutive Cas9 expression might be toxic, similar to what is reported in AML cell lines.¹⁴ Of all the pools tested, the seven B-ALL Cas9-stable pools attaining >75% Cas9 activity were infected with a whole-genome lentiviral 90K sgRNA library (*Online Supplementary Figure S1A and B*).¹⁴ Screen quality was very high, as shown by the BAGEL essential and non-essential genes^{8,15} comparison precision/recall curves (*Online Supplementary Figure 1C*). Furthermore, principal component analysis (PCA) shows that T0 time points from all cell lines are tightly clustered and, despite some variance shown in the Tf between cell lines, cell line replicates were tightly clustered and significantly different from T0, suggesting that significant dropout was achieved in the Tf samples (*Online Supplementary Figure S1D*).

Whole-genome CRISPR screens identify vulnerabilities specific to B-acute lymphoblastic leukemia

In an attempt to identify essential gene unique to B-ALL, we compared the essential genes identified in the screened B-ALL cell lines with the list of essential genes reported in previous datasets. We noticed a considerable overlap of B-ALL essential genes with Broad and Sanger core essential genes⁷ (Figure 1B and C; *Online Supplementary Tables S3 and S4*). One thousand two hundred and four essential genes were identified in at least four of seven B-ALL cell lines (false discovery rate [FDR] <0.05), of which 67% and 63% were also included in the Broad and Sanger gene lists, respectively and, as expected, belong to core biological processes such as the cell cycle, mRNA translation, splicing, and polymerase II transcription pathways that are vital for growth and survival of most cell lines. Strikingly, 72 genes were identified as essential in every B-ALL cell line screened but were not previously identified as essential genes in the Broad and Sanger datasets (Figure 1B, green line). Likewise, 98 genes were previously defined as essential in both the Sanger and Broad dataset but were not essential in any of the ALL cell lines (Figure 1B, red line). We defined as “B-ALL-enriched essential genes” all hits that were found in at



Continued on following page.

Figure 1. Whole-genome CRISPR/Cas9 screens of acute lymphoblastic leukemia (ALL) cell lines identify ALL essential genes. (A) Schema of B-ALL screening pipeline. (B) Significant genes set intersection of 7 B-ALL cell line CRISPR screen results with UpSet, “Broad” and “Sanger” essential gene list at false discovery rate (FDR) <0.05. The intersections with more than 5 genes are shown. (C) Overlap between B-ALL essential (>4/7 cell lines, FDR <0.05) genes, “Broad” and “Sanger” core essential genes. (D) Representative Volcano plot of 697 cells CRISPR screen results with FDR <0.05. B-ALL-known dependencies and B-ALL-enriched essential genes are highlighted in dark blue and in light blue, respectively. Genes regulating ferroptosis induction are highlighted in orange. (E) Gene Network Analysis of B-ALL-enriched essential genes where nodes represent genes and edges represent protein-protein interactions between genes. Node color represents the number of ALL cell lines essential for the given gene. (F) Log₂ fold change distribution of single-guide RNA (sgRNA) in the 7 ALL screened cell lines. sgRNA log₂ fold change for ferroptosis related genes are illustrated at bottom of the panel. VAX1, negative control. TP53 was enriched in several B-ALL cell lines. Tf: final time points; M.O.I: multiplicity of infection.

least four of seven of B-ALL cell lines, but that were not present in the Broad or Sanger essential gene datasets (a total of 319 genes as shown in Figure 1C). These genes are enriched for ALL-associated transcription factors, such as *PAX5*, *EBF1*, *CBFB*, *TCF3*, and *RUNX1*,^{16–18} B-cell receptor and signaling, such as *CD79A*, *CD79B* and *PIK3CD*, and other known B-cell vulnerabilities, such as *CDK6*, *CCND3*, and *BCL2*^{22–24} (Figure 1D). A few genes were also enriched in screened ALL cell lines, such as *TP53* (most B-ALL cell lines have wild-type *TP53*) and *TBC1D4*, indicating that knockout (KO) of these genes provided a proliferative advantage (Figure 1D and F; *Online Supplementary Table S3*). Mapping the “B-ALL-enriched essential genes” onto the STRING database revealed that these genes were members of specific functional subnetworks with multiple protein-protein interactions (Figure 1E), such as *RUNX1*-transcriptional regulation, iron-sulfur cluster assembly, and regulation of lipid metabolism genes. WikiPathway enrichment analysis also identified glutathione metabolism, one carbon metabolism and pentose phosphate pathways, all of which would impact ferroptosis, and ferroptosis regulation itself as specific pathways for B-ALL cell survival (*Online Supplementary Table S5*). Ferroptosis is an iron-dependent form of necrosis which is triggered via lipid peroxidation of polyunsaturated fatty acid (PUFA) at the cell membrane²⁵ and has garnered significant interest in the past few years as an alternative drug-induced cell death mechanisms to therapy-induced apoptosis-resistant cancers.⁹ Central to this cell death pathway is GPX4, one of the top-ranked essential gene according to our screen results (Figure 1D and F; *Online Supplementary Figure S1E*; *Online Supplementary Table S3*) and is the main inhibitor of ferroptosis induction. Interestingly, multiple genes potentially impacting GPX4 activity were included in “B-ALL-enriched essential genes” list (Figure 1F). Hence, our whole-genome screens of B-ALL cell lines identified several genes unique to this histotype and enriched for specific functional pathways, several of which could directly impact ferroptosis induction.

B-acute lymphoblastic leukemia cells are extremely sensitive to ferroptosis induction

GPX4, a selenocysteine-containing glutathione peroxidase, reduces phospholipid hydroperoxides to lipid alcohol with

the help of glutathione (GSH) as an obligate cofactor and acts as the main endogenous inhibitor of ferroptosis induction.²⁶ In order to validate that inhibition of GPX4 induces ferroptosis in ALL cells, we treated cells with RSL3, a direct inhibitor of GPX4.²⁶ Comparison of dose-response curves in B-ALL to non-ALL and GPX4 non-essential cell lines (A549, MCF7, NCIH226) indicates that B-ALL cell lines are particularly sensitive to RSL3 treatment (Figure 2A). This sensitivity was significantly higher compared to the RSL3 sensitivity of many other cell lines reported in previous studies.^{12,27} In order to confirm that RSL3 treatment induces ferroptosis but not apoptosis, we stained ALL cells with C11 BODIPY™, which stains peroxidized lipids, and Annexin V, respectively (*Online Supplementary Figure 2SA*). Lipid peroxidation, but not Annexin V staining, was only detected in the RSL3-treated cells (*Online Supplementary Figure 2A*). Notably, higher lipid peroxidation levels were also found in steady-state conditions in B-ALL cells compared to non-ALL cells (*Online Supplementary Figure 2SB*). In order to confirm the sensitivity of ALL to ferroptosis induction genetically, we generated GPX4 KO clones using CRISPR/Cas9 by constantly growing targeted cells in the presence of ferrostatin-1, a radical trapping agent, which strongly inhibits ferroptosis (Figure 2B and C).^{25,27} Withdrawal of the drug in GPX4 KO clones led to cell death within 18 h after removal, which confirms the rapid induction of cell death after GPX4 inhibition in B-ALL cells (Figure 2B). RSL3 drug treatment could partially be rescued by the iron chelator deferoxamine (DFO), as well as PD146176, a 15-lipoxygenase inhibitor, and EUK-134, a general antioxidant (Figure 2D), but not with Z-VAD-FMK, a pan-inhibitor of caspases and apoptosis. These results indicate that RSL3 creates a lethal oxidative stress environment that is, to some extent, iron-dependent. Interestingly, only lower DFO concentration that was previously reported could rescue cell viability.^{25,27,28} This discrepancy can be explained by the fact that B-ALL cells are more sensitive to elevated DFO treatment (*Online Supplementary Figure 2C*), which could reflect their higher requirement for iron for sustained proliferation compared to other normal cell types and malignancies.²⁹

B-acute lymphoblastic leukemia cells are sensitive to perturbations in pathways regulating GPX4 activity

Because of its requirement for specific cellular metabolites,

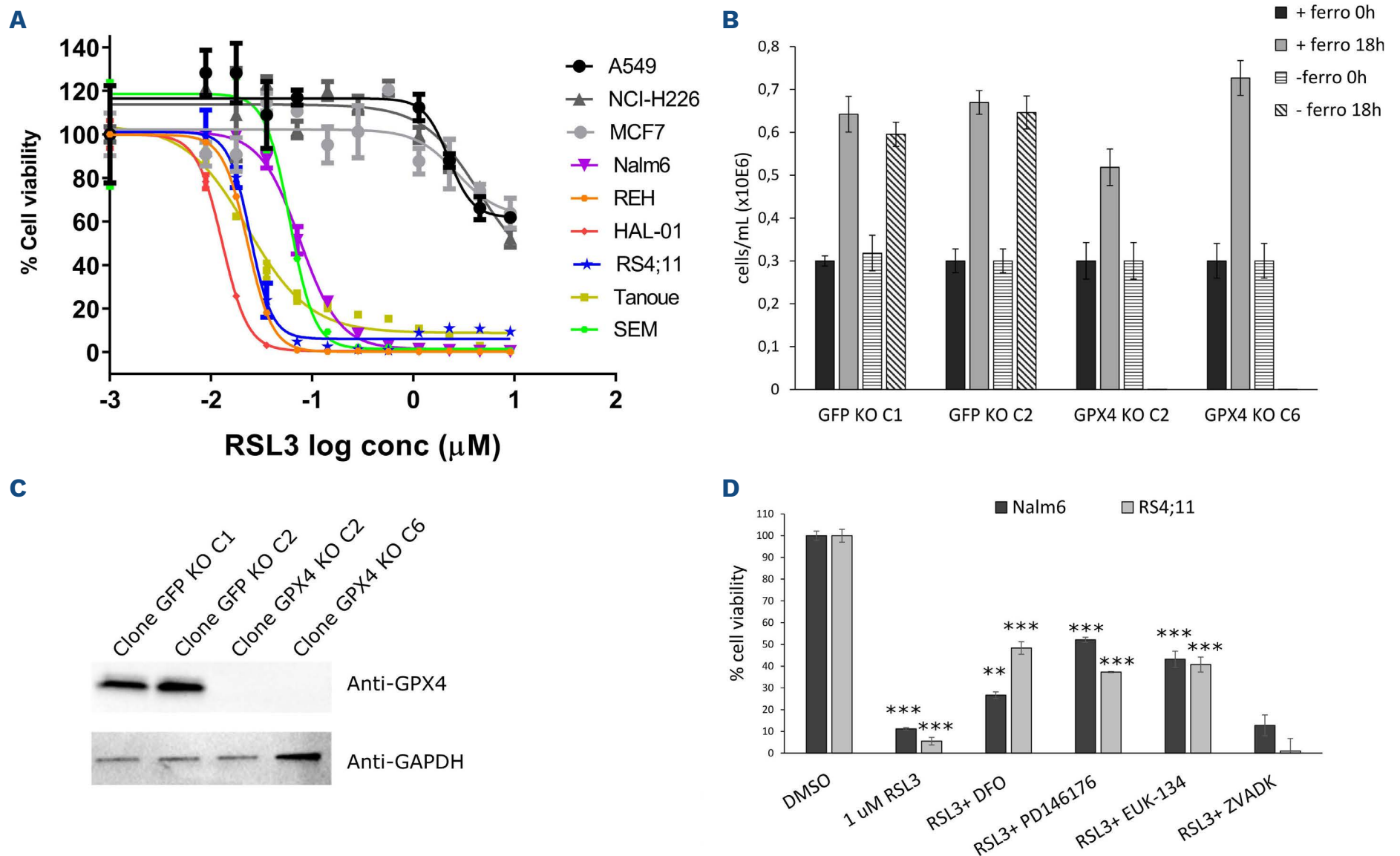
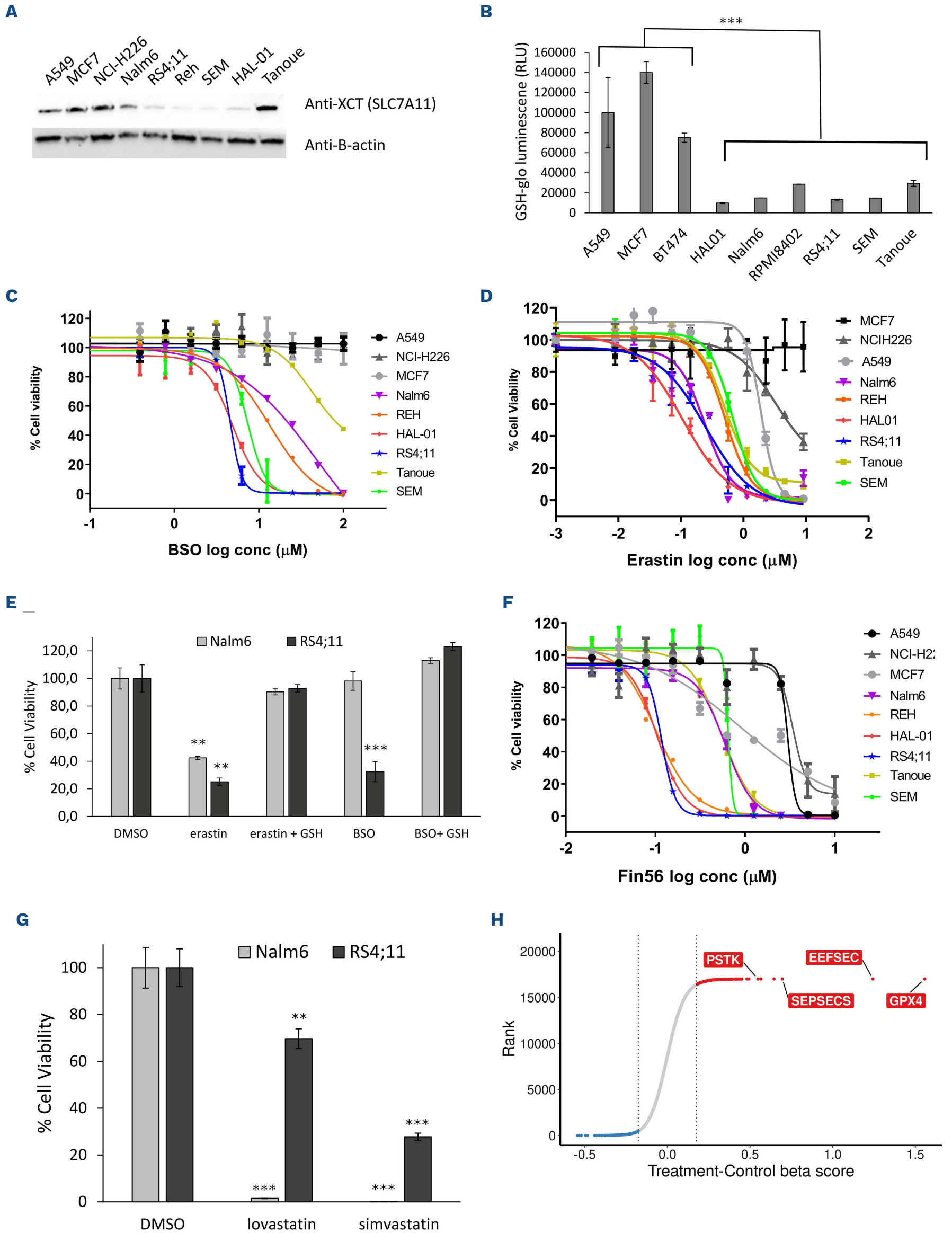


Figure 2. B-acute lymphoblastic leukemia are highly sensitive to GPX4 inhibition. (A) Cell viability curves of B-acute lymphoblastic leukemia (B-ALL) (various colors) and other cell lines (gray colors; A549, MCF7, NCI-H226) to the GPX4 inhibitor (RSL3). (B) Growth of REH GFP clones 1 and 2 (negative control) and REH GPX4 knockout (KO) clones 2 and 6 +/- ferrostatin (2 μ M) for 18 hours (h). (C) Western blot analysis of GPX4 protein level in GPX4 KO vs. GFP KO clones. (D) RSL3 (1 μ M) rescue experiments with the iron chelator deferoxamine (DFO; 10 μ M), the pan-caspase apoptotic inhibitor ZVADK (50 μ M), the 15-lipoxygenase-1 inhibitor PD146176 (0.5 μ M), or the superoxide dismutase mimetic EUK-134 (30 μ M) in NALM6 and RS4;11 for 24 h. **Unpaired *t*-test $P < 0.001$ and *** $P < 0.0001$, where P values for RSL3 treated cells were calculated vs. dimethyl sulfoxide (DMSO)-treated cells and where P values for RSL3 + additives were calculated with RSL3-treated cells. Conc: concentration.

GPX4 activity and ferroptosis induction are influenced by many metabolic pathways.⁹ Several genes regulating these pathways were identified within B-ALL-enriched essential genes (Figures 1F and 6). These include genes implicated in the synthesis of GSH (SLC7A11/SLC3A2/GCLC), mevalonate (HMGCR/MVD/MVK), lipids (ASCL3/4, FASN, MCAT), seleno-compounds (SEPSEC, EEFSEC, SEPHS2), and iron metabolism (PCPB2, TFRC, STEAP3).

Interestingly, most B-ALL cells showed significantly lower levels of SLC7A11 and GSH compared to non-ALL cells, in steady-state conditions (Figure 3A and B). Because of its essential role for GPX4 activity and in oxidative stress protection, low GSH levels could contribute to the increased sensitivity of B-ALL to ferroptosis induction. Accordingly, B-ALL cell lines, with the exception of NALM6 whose sensitivity was intermediate, were more sensitive to buthionine sulfoximine (BSO), a glutamate cysteine ligase (GCLC) inhibitor,³⁰ and to erastin (a direct inhibitor of the Xc- transporter responsible for L-cystine import), than non-ALL cell

lines where GPX4 is non-essential (Figure 3C, D and E). Rescue of BSO or treatments in NALM6 and RS4;11 cells by addition of exogenous GSH indicates that GSH synthesis is essential for ferroptosis inhibition in B-ALL lines (Figure 3E). The mevalonate pathway regulates lipid peroxidation by two different mechanisms. First, it produces CoQ10, which contributes to detoxification of lipid reactive oxygen species (ROS).³¹ Second, it regulates the production of Isopentenyl pyrophosphate (IPP), a metabolite required for Sec-tRNA (a transfer RNA depositing selenocysteine on proteins) synthesis.³¹ Since GPX4 contains a selenocysteine residue essential for ferroptosis inhibition,³² regulation of selenocysteine incorporation into GPX4 can directly influence its activity. B-ALL cells were more sensitive to inhibition of the mevalonate pathway using FIN56, a dual inhibitor of squalene synthase (an enzyme involved in cholesterol biosynthesis)³³ and GPX4 in contrast to non-ALL cells (Figure 3F; *Online Supplementary Figure 3A*). Consistent with these observations, treatments of B-ALL cells



Continued on following page.

Figure 3. Pathways controlling GPX4 activity contribute to acute lymphoblastic leukemia sensitivity. (A) Western blot anti-SLC7A11 in B-acute lymphoblastic leukemia (B-ALL) cell lines. β -actin is used as loading control. (B) GSH level measurement in steady-state conditions for ALL vs. non-GPX4 sensitive (non-ALL) cells. ***Unpaired *t*-test $P < 0.0001$. (C) Half maximal inhibitory concentration (IC_{50}) curves of BSO in ALL cell lines vs. non-GPX4 sensitive (non-ALL, gray tone colors) cell lines after 96-hour (h) treatment. Data shown are from one representative experiment. (D) IC_{50} curves of erastin (system Xc⁻ transporter inhibitor) in ALL vs. non-GPX4 sensitive (non-ALL, gray tone colors) cells. Data shown are from one representative experiment. (E) 10 μ M erastin- and 100 μ M BSO-treated NALM6 and RS4;11 are rescued by 1 mM GSH (48 h). *** Unpaired *t*-test $P < 0.001$ and ** $P < 0.01$. (F) IC_{50} curves of Fin56 inhibitor in ALL vs. non-GPX4 sensitive (non-ALL, gray tone colors) cells. Data shown are from 1 representative experiment. (G) Cell viability of NALM6 and RS4;11 following treatment with lovastatin (20 μ M) and simvastatin (20 μ M) for 72 h. *** Unpaired *t*-test $P < 0.002$ and ** $P < 0.01$. (H) β scores for +/- ferrostatin rescue screens performed in REH^{cas9} and SEM^{cas9} pools. Only GPX4 and selenocompound metabolism genes are indicated. Values represent \log_2 fold change between untreated (control) and treated samples. Conc: concentration.

with other mevalonate pathway inhibitors (lovastatin, simvastatin) also induced cell death (Figure 3G).

In an attempt to determine which genes identified as essential in our primary screens dropped out of the pool specifically because of ferroptosis induction, we performed whole-genome CRISPR screens in two Cas9-expressing B-ALL cell lines in the presence or absence of ferrostatin-1 (*Online Supplementary Figure S3B*; *Online Supplementary Table S6*). In this setting, we would expect genes depleted in the untreated group because of ferroptosis induction to no longer being depleted in the ferrostatin-treated group. As expected, GPX4 sgRNA were no longer depleted in the presence of ferrostatin-1 and showed the highest fold change between untreated and treated samples (Figure 3H). Furthermore, three genes implicated in selenocysteine synthesis (*PSTK*, *EEFSEC* and *SEPSECS*) were also in the top hits further arguing that selenocysteine levels regulate ferroptosis in B-ALL cells (Figure 3G; *Online Supplementary Table S6*). Cells in which these genes were individually knocked out using CRISPR/Cas9 also showed increased lipid peroxidation (*Online Supplementary Figure S3C*), strongly supporting ferroptosis induction. These results are consistent with DepMap CRISPR screen data. By segregating cell lines as GPX4 essential or GPX4 non-essential using the CRISPR screens data (*Online Supplementary Figure S3D*, see materials and methods) and looking for genes that are co-essential with GPX4, we observed co-essentiality of *SEPSECS*, *SEPHS2*, *EEFSEC*, *PSTK* and *SECISBP2* genes (*Online Supplementary Figure S3E*), which are all selenocompound metabolism genes.

B-acute lymphoblastic leukemia cells express low levels of FSP1, a potent ferroptosis inhibitor

Distribution of GPX4 mRNA expression and protein levels between GPX4-sensitive and non-sensitive cell lines in the DepMap/CLE indicate that GPX4 expression level does not account for GPX4 essentiality in cells (*Online Supplementary Figure S4A, B and C*). When looking at differentially expressed genes between these two groups we noticed that *FSP1/AIFM2*, a recently characterized ferroptosis inhibitor,^{12,13} was expressed at lower levels in cells that were dependent on GPX4 compared to non-GPX4 essential cells (*Online Supplementary Figure S4D*). A similar trend was also seen

at the protein level (Figure 4A). Moreover, mRNA and protein levels of FSP1 were particularly low in leukemia cell lines and could not be detected by western blot (Figure 4A and B; *Online Supplementary Figure S4D*). Thus, this low FSP1 level could potentially contribute to the acute vulnerability of B-ALL cells to ferroptosis induction. In order to test this hypothesis, we generated B-ALL stable pools that overexpressed FSP1 (Figure 4B) and compare their RSL3 dose-response curve with parental cells (Figure 4C). Both pools (low or high) overexpressing FSP1 rescued sensitivity to RSL3 treatment by approximately ten-fold compared with parental cell lines, suggesting that the low endogenous constitutive levels of FSP1 contribute to the ferroptosis sensitivity in B-ALL. Furthermore, rescue levels being independent of FSP1 overexpression level indicate that weak overexpression is sufficient to inhibit ferroptosis.

Primary B-acute lymphoblastic leukemia patient-derived xenograft samples are also sensitive to ferroptosis induction *in vitro*

In order to validate that the sensitivity observed in B-ALL cell lines is conserved in PDX samples, we tested different ferroptosis-inducing drugs on nine B-ALL PDX having only gone through a single round of amplification in mice previous to these tests. All PDX samples showed high sensitivity to RSL3 treatment and were even more sensitive than the positive control cell lines, NALM6 (Figure 5A). Furthermore, ferrostatin-1 treatment rescued RSL3 sensitivity in all PDX, indicating that ferroptosis is the major cell death mechanism in these RSL3-treated PDX. B-ALL PDX were also sensitive to three other ferroptosis-inducing drugs - erastin, FIN56 and sulfasalazine - although all PDX were not necessarily sensitive to all drugs (Figure 5B to D). Erastin and sulfasalazine demonstrated a similar sensitivity profile consistent with these two drugs targeting the Xc⁻ transporter. In all, these experiments confirm the extreme sensitivity of B-ALL cell lines and PDX samples to ferroptosis induction.

Discussion

Despite the continuous improvement in treatment outcome and the greater understanding of the molecular pa-

thogenesis underlying tumor development, B-ALL still poses unresolved clinical needs, especially to relapsed patient. Developing additional therapeutic avenues by identifying new vulnerabilities is therefore critical to provide new strategies for cancer treatment. In an attempt to fulfill this gap, we performed whole-genome pooled dropout CRISPR screens in B-ALL cell lines. These screens found essential genes that were mostly shared with other cancer histotypes; these genes were enriched in core essential

genes mostly implicated in general processes such as transcription, translation, proteasome, etc. In addition, these screens also identified a panel of more than 300 genes that were essential in most ALL cell line, but not across other tumor histotypes,⁷ suggesting that these genes represent unique functional vulnerabilities to B-ALL. These were enriched for well-described B-ALL specific transcription factors (*PAX5*, *RUNX1*, *TCF3*, *EBF1*) and signal transduction pathways (*CD79A*, *CD79B*, *PIK3CD*), but also

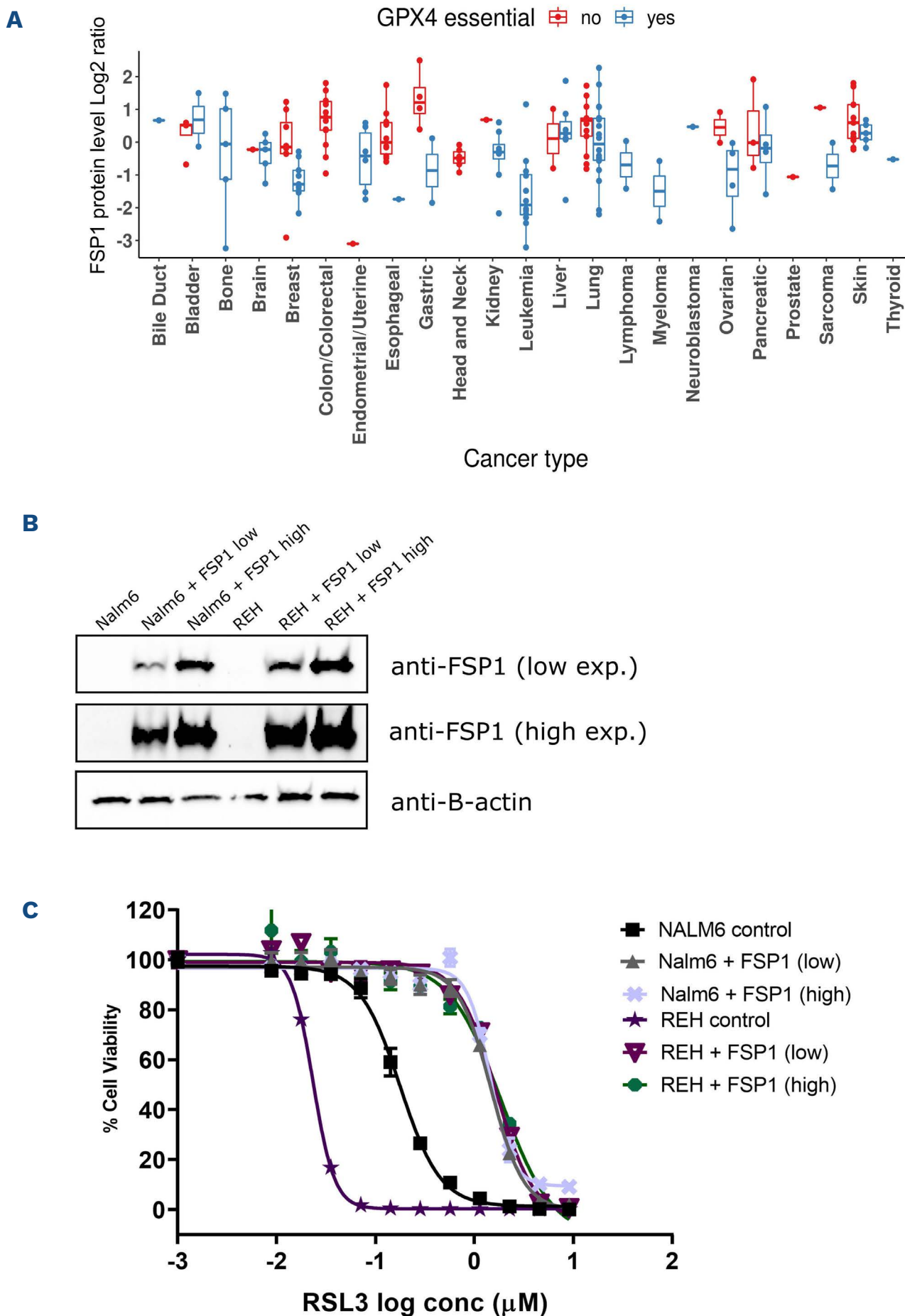


Figure 4. Low level of FSP1 in B-acute lymphoblastic leukemia contributes to ferroptosis sensitivity. (A) FSP1 protein level comparison between GPX4-sensitive and non-sensitive CCLE cell lines by cancer type (see material and methods). (B) FSP1 western blot on parental vs. FSP1 over-expressing B-acute lymphoblastic leukemia (B-ALL) cells. β -actin is shown as a loading control. (C) RSL3 dose-response curves in B-ALL pools overexpressing high or low levels of FSP1. Conc: concentration.

novel vulnerabilities not previously linked to B-ALL, several of which directly regulate ferroptosis induction.

Ferroptosis is a recently described iron-dependent cell death pathway that is characterized by the excessive peroxidation of phospholipid at the cell membranes. This non-apoptotic cell death pathway has garnered increasing interest as a potential novel cancer therapy since “persister” cells rendered drug-tolerant through serial exposure to chemotherapeutic agents and cells that underwent an epithelial-mesenchymal transition, two states associated with resistance to cancer therapy, demonstrate exquisite sensitivity to ferroptosis induction.^{27,34}

The main gatekeeper for ferroptosis induction is GPX4, a glutathione peroxidase, which uses GSH as an obligate co-factor and possess the unique ability to detoxify hydroperoxides in complex lipids. Our findings add B-ALL lines to the cell lines or cell state that have been reported to be sensitive to GPX4 inhibition by either ferroptosis inducing drug^{12,26,27} or direct gene KO.³⁵ To our knowledge, this is the first evidence of such a sensitivity in these cells. Many genes modulating ferroptosis induction are still not labeled as such by KEGG or MSigDB enrichment tools,^{36–38} especially for genes involved in the multiple metabolic pathways that are indirectly regulating GPX4 activity (Fi-

gure 6). This explains why ferroptosis pathway, even if significantly enriched, was not ranked higher in our Wikipathway analysis (*Online Supplementary Table S5*) even though many B-ALL essential genes were involved in pathways related to GPX4 activity, such as selenocompound, lipid, mevalonate, GSH and iron metabolism (Figure 6). We validated several of these genetic dependencies using orthogonal assays and demonstrated that inhibition of these pathways induce ferroptosis in B-ALL cells. As seen in the +/- ferrostatin-1 screens, apart from GPX4, B-ALL cells were also particularly sensitive to the depletion of genes implicated in selenocysteine synthesis (Figure 3H). Selenocysteine incorporation into GPX4 is required for its ferroptosis inhibitor activity³² and co-essentiality of selenocysteine synthesis genes with GPX4 was previously demonstrated in glioblastoma cells.³⁹ These results also suggest that the primary role of selenocysteine metabolism in ALL cells is to synthesize GPX4 as none of the 24 other selenocysteine-containing proteins were essential in our screen. This is reminiscent of genetic deletion of selenocysteine-containing proteins in mice where KO of *GPX4* is the only one that is embryonic lethal, a phenotype shared with selenocysteine tRNA KO mice.^{40,41} Several elements seem to synergize to explain the high

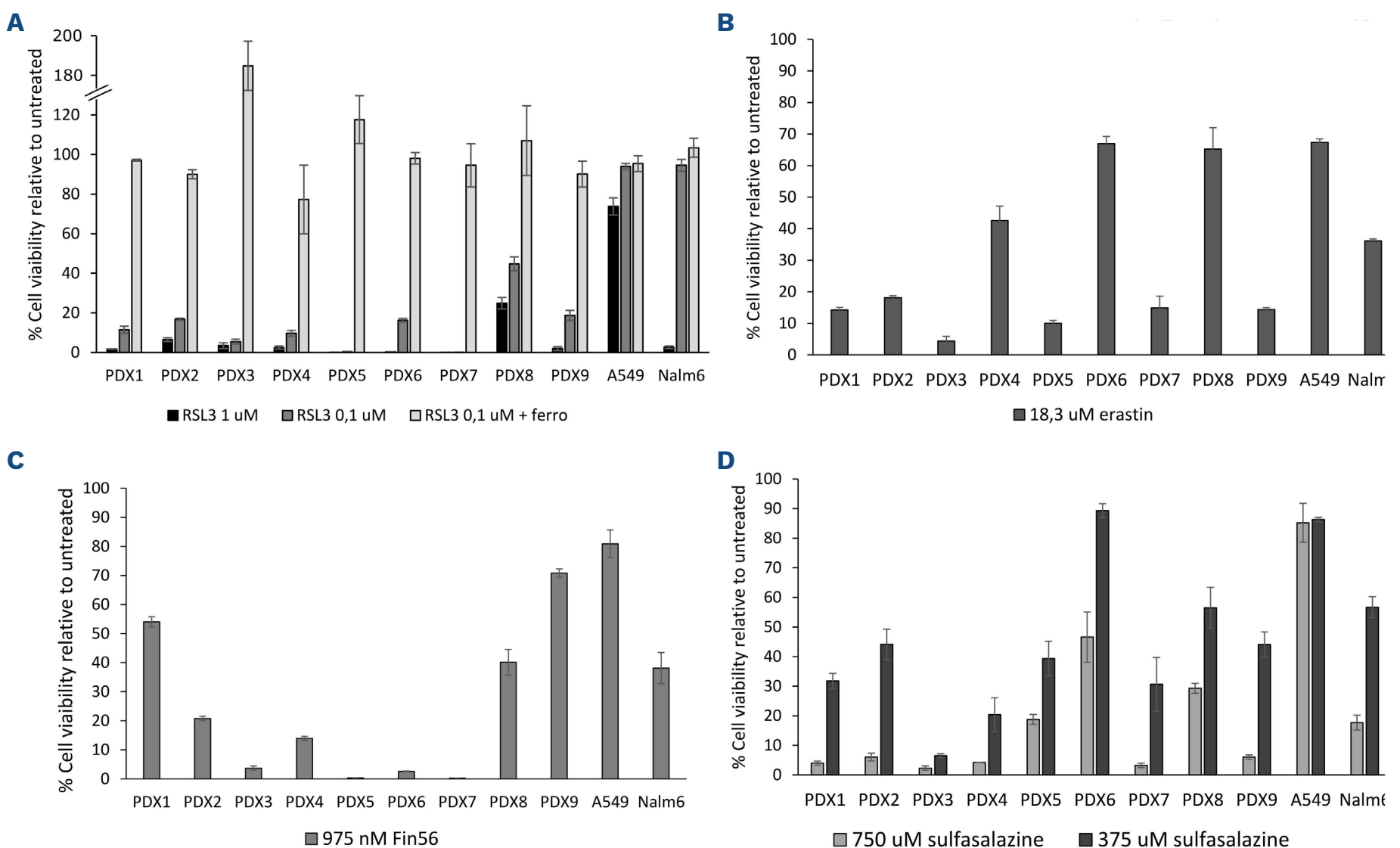


Figure 5. B-acute lymphoblastic leukemia patient-derived xenografts are sensitive to ferroptosis inducing drugs *in vitro*. B-acute lymphoblastic leukemia (B-ALL) patient-derived xenografts were treated with (A) RSL3 +/- ferrostatin (ferro), (B) erastin, (C) Fin56, and (D) sulfasalazine. Cell viability was assessed 36 hours post treatment and compared to untreated xenografts.

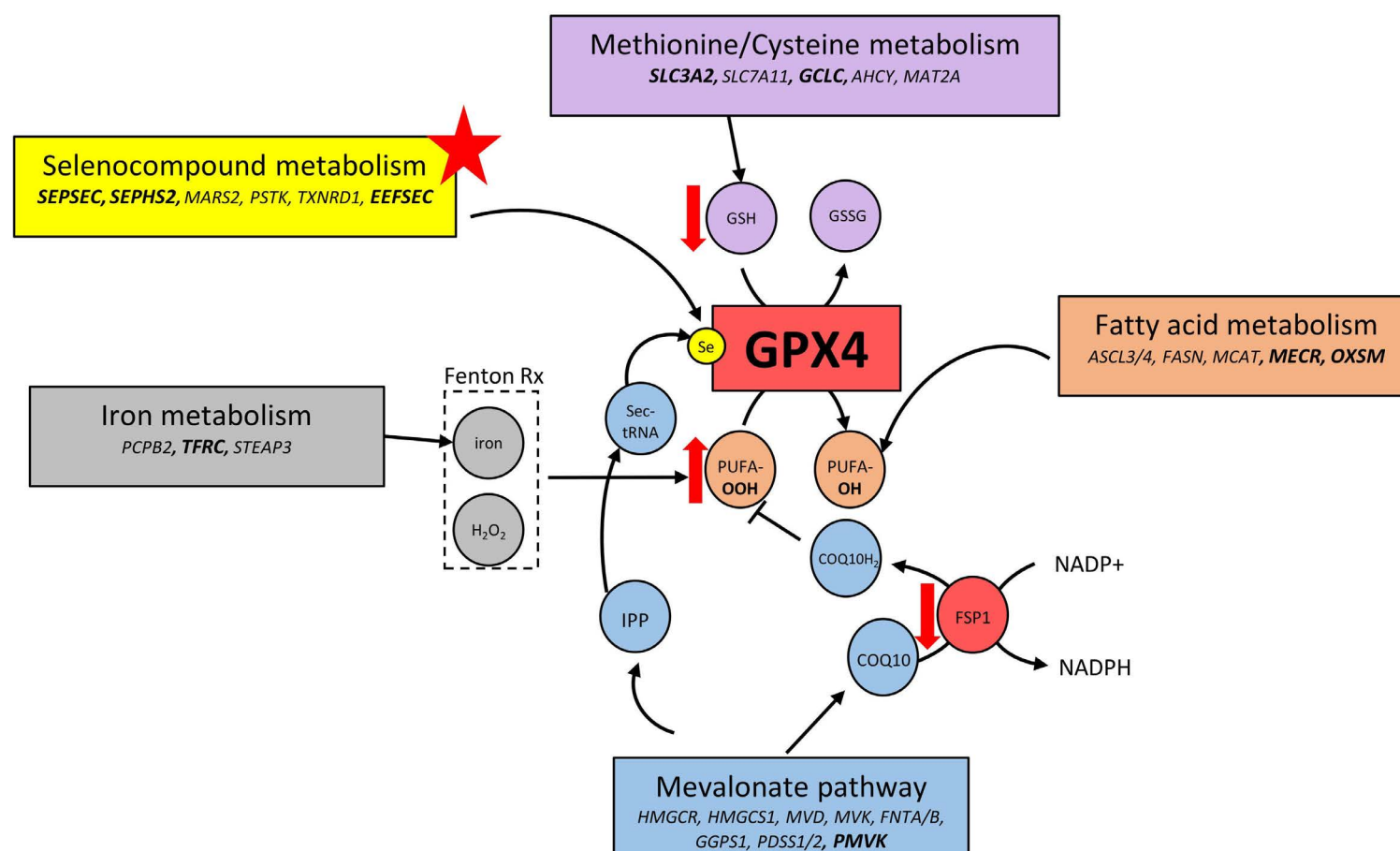


Figure 6. Integration of GPX4-related pathways. Several genes/pathways found essential in acute lymphoblastic leukemia (ALL) cells potentially regulate GPX4 activity which may explain their acute vulnerability to ferroptosis induction. Genes in bold characters are found within the 319 ALL-enriched essential genes.

sensitivity of B-ALL cells to ferroptosis induction. High lipid ROS levels in steady-state conditions suggest that B-ALL are under constant oxidative stress. Combined with the low GSH and FSP1 antioxidant levels, it implies that these cells do not possess the buffering capacity that would normally protect them against oxidative stress. And while restoring FSP1 expression levels in B-ALL cell increases resistance to ferroptosis induction (Figure 4C), this only partially rescues sensitivity compared to other resistant cell lines, suggesting that additional elements contribute to the extreme sensitivity of B-ALL cells to ferroptosis induction. One explanation might lie in the high levels of PUFA that were measured in B-ALL⁴² since a direct correlation between PUFA levels in cell lines and *GPX4* KO sensitivity has been established by metabolite dependency association studies.⁴³ In addition, transcriptional repression of the pentose phosphate pathway (PPP) by B-cell-specific transcriptional factor PAX5 and IKZF1 in B-ALL limits its activity and ability to cope with oxidative stress.⁴⁴ This particular vulnerability results in low levels of NADPH, which prevents GSSG reduction into GSH. The limited PPP activity appears to be controlled both by the serine-threonine protein phosphatase 2A (PP2A) and the Cyclin D3-CDK6 kinase; inhibition of the latter reduces the flow of carbon through the PPP in favor of glycolysis.⁴⁵ Cyclin D3-CDK6 kinase regulates the switch from glycolysis to the PPP by directly phosphorylating and inhibiting key enzymes, which catalyze key rate-limiting steps in the glycolysis cascade such as 6-phosphofructokinase (PFK1), py-

ruvate kinase M2 (PKM2), but also GPI, PGK1, ENO1, and PKM. Notably, the last four enzymes along with Cyclin D3 (CCND3) and CDK6 are all considered “B-ALL-enriched essential genes” according to our screens. Overall, these results, along with the one presented in this paper, suggest that the low PPP activity found in B-ALL, which leads to low levels of NADPH and GSH, restricts their ability to cope with oxidative stress. This strenuous balance can be easily tipped toward ferroptosis induction when GPX4 is inhibited. Because B-ALL are primed to undergo ferroptosis and multiple metabolic pathways modulate GPX4 activity, several therapeutic opportunities are potentially available to target this vulnerability. As shown by our results and others, ALL cells are also sensitive to drugs such as sulfasalazine (Figure 5D), BSO (Figure 3A), and statins (Figure 3E and ⁴⁶), which have all been previously used in clinical setting. However, these drugs do not directly target ferroptosis inhibitors such as GPX4 or FSP1, but mainly induce ferroptosis by targeting pathways that incidentally influence sensitivity to ferroptosis induction (lipid metabolism, GSH metabolism, etc). No highly potent bioavailable drug directly targeting ferroptosis inhibitors currently exist, which severely limits the therapeutic validation of this pathway *in vivo*. IKE, an erastin derivative, has been specifically modified to increase bioavailability *in vivo*.⁴⁷ Despite this, pharmacokinetic and biodistribution of the drug showed a very short half-life *in vivo* (less than 2 hours) and a low achievable concentrations in the blood.⁴⁷ Moreover, caution should be taken

in developing novel ferroptosis inhibitors for cancer treatment, as ferroptosis has been implicated in neuropathologies development and neurotoxicity,^{48–51} as well as cardiomyopathies.⁵² Since many chemotherapies have been shown to induce oxidative stress in cancer cells, combining these treatments with a ferroptosis inducing agent could help prevent the development of treatment-resistant tumor cells. Finally, according to gene/protein expression analyses, other leukemias, such as T-ALL and acute myeloid leukemia (AML), also share a similar expression profile for gene controlling sensitivity to ferroptosis induction and would also likely benefit from therapeutic strategies developed for ALL. In fact, RSL3 sensitivity was previously reported for two T-ALL cell lines,⁵³ and recently, AML cell lines and PDX were shown to be sensitive to ferroptosis induction using APR-246, a p53 activating drug.⁵⁴ Overall, our work identified a comprehensive set of genetic dependencies and molecular mechanisms sustaining tumorigenesis in B-ALL cell lines, some of which could potentially be further exploited therapeutically.

Disclosures

No conflicts of interest to disclose.

References

- Sabattini E, Bacci F, Sagrmoso C, Pileri SA. WHO classification of tumours of haematopoietic and lymphoid tissues in 2008: an overview. *Pathologica*. 2010;102(3):83–87.
- Ellison LF, De P, Mery LS, Grundy PE, for the Canadian Cancer Society's Steering Committee for Canadian Cancer Statistics. Canadian cancer statistics at a glance: cancer in children. *Can Med Assoc J*. 2009;180(4):422–424.
- Vrooman LM, Silverman LB. Treatment of childhood acute lymphoblastic leukemia: prognostic factors and clinical advances. *Curr Hematol Malig Rep*. 2016;11(5):385–394.
- Bruzzi P, Bigi E, Predieri B, et al. Long-term effects on growth, development, and metabolism of ALL treatment in childhood. *Expert Rev Endocrinol Metab*. 2019;14(1):49–61.
- Meyers RM, Bryan JG, McFarland JM, et al. Computational correction of copy number effect improves specificity of CRISPR–Cas9 essentiality screens in cancer cells. *Nat Genet*. 2017;49(12):1779–1784.
- Behan FM, Iorio F, Picco G, et al. Prioritization of cancer therapeutic targets using CRISPR–Cas9 screens. *Nature*. 2019;568(7753):511–516.
- Dempster JM, Pacini C, Pantel S, et al. Agreement between two large pan-cancer CRISPR–Cas9 gene dependency data sets. *Nat Commun*. 2019;10(1):5817.
- Hart T, Chandrashekar M, Aregger M, et al. High-resolution CRISPR screens reveal fitness genes and genotype-specific cancer liabilities. *Cell*. 2015;163(6):1515–1526.
- Hassannia B, Vandenabeele P, Vanden Berghe T. Targeting ferroptosis to iron out cancer. *Cancer Cell*. 2019;35(6):830–849.
- Jiang X, Stockwell BR, Conrad M. Ferroptosis: mechanisms, biology and role in disease. *Nat Rev Mol Cell Biol*. 2021;22(4):266–282.
- Wang L, Chen X, Yan C. Ferroptosis: an emerging therapeutic opportunity for cancer. *Genes Dis*. 2020;9(12):334–346.
- Doll S, Freitas FP, Shah R, et al. FSP1 is a glutathione-independent ferroptosis suppressor. *Nature*. 2019;575(7784):693–698.
- Bersuker K, Hendricks JM, Li Z, et al. The CoQ oxidoreductase FSP1 acts parallel to GPX4 to inhibit ferroptosis. *Nature*. 2019;575(7784):688–692.
- Tzelepis K, Koike-Yusa H, De Braekeleer E, et al. A CRISPR dropout screen identifies genetic vulnerabilities and therapeutic targets in acute myeloid leukemia. *Cell Rep*. 2016;17(4):1193–1205.
- Hart T, Moffat J. BAGEL: a computational framework for identifying essential genes from pooled library screens. *BMC Bioinformatics* 2016;17(1):164.
- Metzeler KH, Bloomfield CD. Clinical relevance of RUNX1 and CFBF alterations in acute myeloid leukemia and other hematological disorders. *Adv Exp Med Biol*. 2017;962:175–199.
- Gu Z, Churchman ML, Roberts KG, et al. PAX5-driven subtypes of B-progenitor acute lymphoblastic leukemia. *Nat Genet*. 2019;51(2):296–307.
- Hein D, Borkhardt A, Fischer U. Insights into the prenatal origin of childhood acute lymphoblastic leukemia. *Cancer Metastasis Rev*. 2020;39(1):161–171.
- Chu PG, Arber DA. CD79: a review. *Appl Immunohistochem Mol Morphol*. 2001;9(2):97–106.
- Kruth KA, Fang M, Shelton DN, et al. Suppression of B-cell development genes is key to glucocorticoid efficacy in treatment of acute lymphoblastic leukemia. *Blood*. 2017;129(22):3000–3008.
- Serafin V, Porcù E, Cortese G, et al. SYK Targeting represents a potential therapeutic option for relapsed resistant pediatric ETV6–RUNX1 B-acute lymphoblastic leukemia patients. *Int J Mol Sci*. 2019;20(24):6175.

Contributions

MEL and RM designed the study and prepared the manuscript. MEL and AMG performed the experiments. MEL, MS, AMG, JSM, SD and RM analyzed the data. KB and EH provided patient samples. SD managed resource requirements; and all authors edited and approved the manuscript.

Acknowledgments

We thank Sonia Leclerc for performing next-generation sequencing experiments. We also thank Nadine Fradet, Christine Gadoury and Mylène Gosselin for their contribution to early development of the experimental designs. All authors are members of the NRC-CHUSJ Collaborative Unit for Translational Research (CUTR). This is NRC publication # 53536.

Funding

We would like to acknowledge CUTR for funding part of this work.

Data-sharing statement

Raw screen data are available upon request.

22. Bortolozzi R, Mattiuzzo E, Trentin L, Accordi B, Basso G, Viola G. Ribociclib, a Cdk4/Cdk6 kinase inhibitor, enhances glucocorticoid sensitivity in B-acute lymphoblastic leukemia (B-ALL). *Biochem Pharmacol.* 2018;153:230-241.
23. Ott CJ, Kopp N, Bird L, et al. BET bromodomain inhibition targets both c-Myc and IL7R in high-risk acute lymphoblastic leukemia. *Blood.* 2012;120(14):2843-2852.
24. Scheffold A, Jebaraj BMC, Stilgenbauer S. Venetoclax: targeting BCL2 in hematological cancers. *Recent Results Cancer Res.* 2018;212:215-242.
25. Dixon SJ, Lemberg KM, Lamprecht MR, et al. Ferroptosis: an iron-dependent form of nonapoptotic cell death. *Cell.* 2012;149(5):1060-1072.
26. Yang WS, SriRamaratnam R, Welsch ME, et al. Regulation of ferroptotic cancer cell death by GPX4. *Cell.* 2014;156(1-2):317-331.
27. Hangauer MJ, Viswanathan VS, Ryan MJ, et al. Drug-tolerant persister cancer cells are vulnerable to GPX4 inhibition. *Nature.* 2017;551(7679):247-250.
28. Zhang Y, Swanda RV, Nie L, et al. mTORC1 couples cyst(e)ine availability with GPX4 protein synthesis and ferroptosis regulation. *Nat Commun.* 2021;12(1):1589.
29. Wang F, Lv H, Zhao B, et al. Iron and leukemia: new insights for future treatments. *J Exp Clin Cancer Res.* 2019;38(1):406.
30. Griffith OW. Mechanism of action, metabolism, and toxicity of buthionine sulfoximine and its higher homologs, potent inhibitors of glutathione synthesis. *J Biol Chem.* 1982;257(22):13704-13712.
31. Moosmann B, Behl C. Selenoproteins, cholesterol-lowering drugs, and the consequences revisiting of the mevalonate pathway. *Trends Cardiovasc Med.* 2004;14(7):273-281.
32. Ingold I, Berndt C, Schmitt S, et al. Selenium utilization by GPX4 is required to prevent hydroperoxide-induced ferroptosis. *Cell.* 2018;172(3):409-422.
33. Shimada K, Skouta R, Kaplan A, et al. Global survey of cell death mechanisms reveals metabolic regulation of ferroptosis. *Nat Chem Biol.* 2016;12(7):497-503.
34. Viswanathan VS, Ryan MJ, Dhruv HD, et al. Dependency of a therapy-resistant state of cancer cells on a lipid peroxidase pathway. *Nature.* 2017;547(7664):453-457.
35. Tsherniak A, Vazquez F, Montgomery PG, et al. Defining a cancer dependency map. *Cell.* 2017;170(3):564-576.
36. Subramanian A, Tamayo P, Mootha VK, et al. Gene set enrichment analysis: a knowledge-based approach for interpreting genome-wide expression profiles. *Proc Natl Acad Sci U S A.* 2005;102(43):15545-15550.
37. Liberzon A, Birger C, Thorvaldsdóttir H, Ghandi M, Mesirov JP, Tamayo P. The Molecular Signatures Database (MSigDB) hallmark gene set collection. *Cell Syst.* 2015;1(6):417-425.
38. Kanehisa M, Goto S. KEGG: kyoto encyclopedia of genes and genomes. *Nucleic Acids Res.* 2000;28(1):27-30.
39. Kim E, Dede M, Lenoir WF, et al. A network of human functional gene interactions from knockout fitness screens in cancer cells. *Life Sci Alliance.* 2019;2(2):e201800278.
40. Ufer C, Wang CC. The roles of glutathione peroxidases during embryo development. *Front Mol Neurosci.* 2011;4:12.
41. Yant LJ, Ran Q, Rao L, et al. The selenoprotein GPX4 is essential for mouse development and protects from radiation and oxidative damage insults. *Free Radic Biol Med.* 2003;34(4):496-502.
42. Agatha G, Häfer R, Zintl F. Fatty acid composition of lymphocyte membrane phospholipids in children with acute leukemia. *Cancer Lett.* 2001;173(2):139-144.
43. Li H, Ning S, Ghandi M, et al. The landscape of cancer cell line metabolism. *Nat Med.* 2019;25(5):850-860.
44. Xiao G, Chan LN, Klemm L, et al. B-cell-specific diversion of glucose carbon utilization reveals a unique vulnerability in B cell malignancies. *Cell.* 2018;173(2):470-484.
45. Wang H, Nicolay BN, Chick JM, et al. The metabolic function of cyclin D3-CDK6 kinase in cancer cell survival. *Nature.* 2017;546(7658):426-430.
46. Sheen C, Vincent T, Barrett D, et al. Statins are active in acute lymphoblastic leukaemia (ALL): a therapy that may treat ALL and prevent avascular necrosis. *Br J Haematol.* 2011;155(3):403-407.
47. Zhang Y, Tan H, Daniels JD, et al. Imidazole ketone erastin induces ferroptosis and slows tumor growth in a mouse lymphoma model. *Cell Chem Biol.* 2019;26(5):623-633.
48. Zuo Y, Xie J, Li X, et al. Ferritinophagy-mediated ferroptosis involved in Paraquat-induced neurotoxicity of dopaminergic neurons: implication for neurotoxicity in PD. *Oxid Med Cell Longev.* 2021;2021:9961628.
49. Do Van B, Gouel F, Jonneaux A, et al. Ferroptosis, a newly characterized form of cell death in Parkinson's disease that is regulated by PKC. *Neurobiol Dis.* 2016;94:169-178.
50. Guiney SJ, Adlard PA, Bush AI, Finkelstein DI, Ayton S. Ferroptosis and cell death mechanisms in Parkinson's disease. *Neurochem Int.* 2017;104:34-48.
51. Hambright WS, Fonseca RS, Chen L, Na R, Ran Q. Ablation of ferroptosis regulator glutathione peroxidase 4 in forebrain neurons promotes cognitive impairment and neurodegeneration. *Redox Biol.* 2017;12:8-17.
52. Wu X, Li Y, Zhang S, Zhou X. Ferroptosis as a novel therapeutic target for cardiovascular disease. *Theranostics.* 2021;11(7):3052-3059.
53. Probst L, Dächert J, Schenk B, Fulda S. Lipoxigenase inhibitors protect acute lymphoblastic leukemia cells from ferroptotic cell death. *Biochem Pharmacol.* 2017;140:41-52.
54. Birsén R, Larrue C, Decroocq J, et al. APR-246 induces early cell death by ferroptosis in acute myeloid leukemia. *Haematologica.* 2022;107(2):403-416.
55. Szklarczyk D, Gable AL, Lyon D, et al. STRING v11: protein-protein association networks with increased coverage, supporting functional discovery in genome-wide experimental datasets. *Nucleic Acids Res.* 2019;47(D1):D607-D613.
56. Shannon P, Markiel A, Ozier O, et al. Cytoscape: a software environment for integrated models of biomolecular interaction networks. *Genome Res.* 2003;13(11):2498-2504.
57. Chin C-H, Chen S-H, Wu H-H, Ho C-W, Ko M-T, Lin C-Y. cytoHubba: identifying hub objects and sub-networks from complex interactome. *BMC Syst Biol.* 2014;8 (Suppl 4):S11.
58. Wang B, Wang M, Zhang W, et al. Integrative analysis of pooled CRISPR genetic screens using MAGeCKFlute. *Nat Protoc.* 2019;14(3):756-780.